Table 1 Operational drag area vs time

Event	Time, s	C_DS, ft^2
Lid fire	0	11.6
Line stretch	0.4	11.6
15 ft reefed	0.6	45.0
Reef cut	10.4	45.0
15 ft open	10.5	100.0
15 ft release	25.0	100.0
73 ft lines deploy	25.01	11.6
73 ft canopy stretch	25.8	11.6
Reef open	32.0	450.0
Reef cut	36.0	450.0
Full open	37.5	2250.0
To impact	1000.0	2250.0

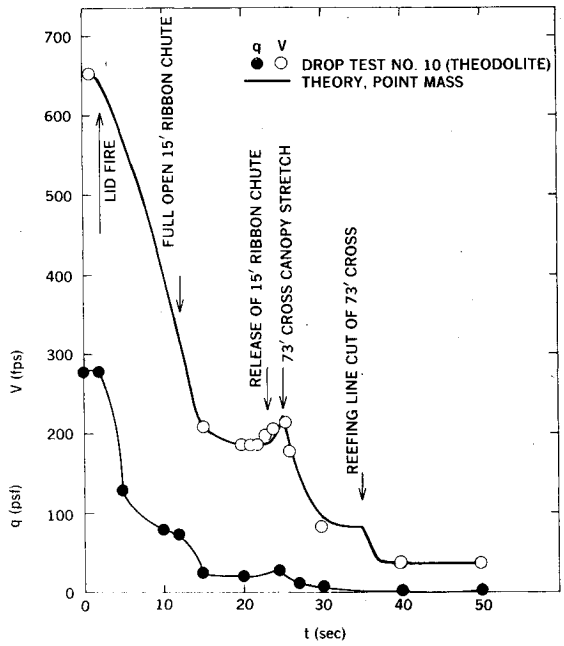

Fig. 2 Velocity and dynamic pressure decay with time after drop.

Analysis of Data

Theoretical point-mass trajectory calculations run on the CDC 7600 computer were used for all the tests. The drag-area variation with time listed in Table 1 was used. A typical comparison (Fig. 2) of theory (solid line) and theodolite tracking data (circles) velocity and dynamic pressure variation with time after release from the A7 aircraft shows excellent agreement for the last drop test.

Parachute peak loads were obtained from point mass theoretical trajectories. First stage suspension line peak load of about 8500 lb is well below the design allowable value of 16,000 lb. The weak link in the system is the two-ply 1.1-oz/yd^2 nylon cloth in the crown of the 73-ft cross. This material is subject to friction burning at the high bag strip velocities.

Conclusions

A series of ten drop tests was conducted to develop a two-stage parachute recovery system for the NASA ARIES space telescope research. The final system consists of a 15-ft-diam ribbon parachute reefed to 50% for 10 s and a 73-ft-diam cross or paraform reefed to 20% for 10 s. The following conclusions were reached: 1) The recovery system is qualified for a 2200-lb payload. 2) Two successful operational flights with recovery of 1600- and 2056-lb payloads were conducted at White Sands Missile Range.

Acknowledgments

The parachutes were rigged and packed by Horace Lucero and Alvin Oleson at the Sandia Parachute Laboratory. This work was supported by the U.S. Department of Energy and the National Aeronautics and Space Administration.

References

[1] Steeves, R.G., "73 Foot Paraform Drop Test Report No.1290-TR-10," Space Vector Corp., Northridge, Calif., Aug. 1979.

[2] Morrison, R.S., "Evaluation of the 73-foot Diameter Paraform Recovery Parachute System," AFFTC-TR-30, Dec. 1979.

[3] Steeves, R.G., "Design Study of a Parachute System for ARIES Payloads," Space Vector Corp., Northridge, Calif., Report 1290-TR-7, May 1979.

AIAA 82-4165

STOL Aircraft Response to Turbulence Generated by a Tall Upwind Building

Lloyd D. Reid*
University of Toronto, Ontario, Canada

Nomenclature

A, B, C	= constant system matrices
h	= height above ground level
h_G	= thickness of the planetary boundary layer
$H(t,t')$	= system state transition matrix
x_i	= position relative to the point where the glideslope intersects the runway
$R(t_1,t_2)$	= turbulence correlation matrix
$R_{W_iW_j}(\tau)$	= ijth element of $R(t_1,t_2)$
t	= time
t_i	= time at which aircraft reaches position x_i
W	= wind velocity
W_G	= wind velocity at the top of the planetary boundary layer
W	= turbulence velocity in the atmosphere
(W_1W_2)	= the x and z components of W in an Earth-fixed reference frame
$\mathfrak{X}$	= vector with components X (column matrix)
X	= matrix
X^T	= transpose of X
$\langle x \rangle$	= expected value of x
$\bar{x}$	= mean value of $x(t)$
$\hat{x}$	= root mean square of $x(t)$
Δu	= aircraft's longitudinal airspeed perturbation
Δx	= aircraft state vector
τ	= time delay $(t_2 - t_1)$
$(\dot{})$	= d( )/dt

Introduction

THE prediction of aircraft response to wind shear and turbulence on the landing approach has been addressed by several authors recently. This has been prompted by the occurrence of a number of wind-related fatal accidents and by an interest in downtown STOLport operations. Several

Received Nov. 25, 1981; revision received March 8, 1982.

*Associate Professor, Institute for Aerospace Studies. Associate Fellow AIAA.

analysis methods have been studied, including power spectral density techniques,[1] the equivalent deterministic variable technique,[2] worst-case wind modeling,[3,4] and turbulence correlation techniques.[5,6] A comparison of these methods is presented in Ref. 7. Relatively little work has been reported on predicting the influence on aircraft response of wind disturbances created by man-made structures. A notable exception is the research described in Ref. 8 dealing with building-induced wind shear and its effect on the landing performance of aircraft.

The present paper reports on the application of the turbulence correlation technique to the prediction of the influence of building-induced turbulence on the landing approach of aircraft. This technique is based on a linear theory; hence the concurrent effect of building-induced wind shear can be analyzed separately (e.g., using the results of Ref. 8) and then added to the turbulence response to produce the aircraft's overall response to the wind.

Turbulence Correlation Technique

The turbulence correlation technique is fully described in Refs. 5 and 6. A unique feature of this approach is its ability to handle inhomogeneous and nonisotropic turbulence fields. In the present application, the aircraft response to turbulence is represented by the following linearized equations of motion for perturbations about a reference equilibrium flight condition.

$$\Delta\dot{x} = A\Delta x + BW + C\dot{W} \tag{1}$$

where

$$W^T = (W_1 W_2) \tag{2}$$

The dispersion in the aircraft's state vector about the reference equilibrium flight condition at any time t is given by

$$\langle \Delta x(t)\Delta x^T(t)\rangle \equiv \int_0^t \int_0^t H(t,t_1)R(t_1,t_2)H^T(t,t_2)\,dt_1\,dt_2 + CR(t,t)C^T - C\int_0^t R(t,t')H^T(t,t')\,dt' - \left(C\int_0^t R(t,t')H^T(t,t')\,dt'\right)^T \tag{3}$$

where

$$H(t,t') = [\exp\{(t-t')A\}][-(B+AC)] \tag{4}$$

and

$$R(t_1,t_2) = \overline{W(\tau_1,t)\,W^T(\tau_2,t+\tau)} \tag{5}$$

is the turbulence correlation matrix. In Eq. (5), $W(\tau_i,t)$ represents the time history of the turbulence as measured at the location on the glideslope indicated by the position vector τ_i, which is reached by the aircraft at time t_i and

$$\tau = t_2 - t_1 \tag{6}$$

The value of $H(t,t')$ depends on the aircraft dynamics; and the value of $R(t_1,t_2)$ is found by making appropriate measurements in the atmosphere or in a planetary boundary-layer wind tunnel.

Wind Tunnel Measurements

The goal of the present study was to determine the influence of the turbulence generated by a tall upwind building on the landing approach of a STOL transport. In particular, it was desired to measure the increase in the dispersion of the aircraft's longitudinal state vector over that resulting from the naturally occurring turbulence in the Earth's planetary boundary layer as reported in Ref. 6. The measurements were taken in a planetary boundary-layer wind tunnel (with a cross section of 1.12×1.68 m) having a mean wind velocity profile W given by (in the absence of obstructions)

$$W/W_G = [h/h_G]^{0.16} \tag{7}$$

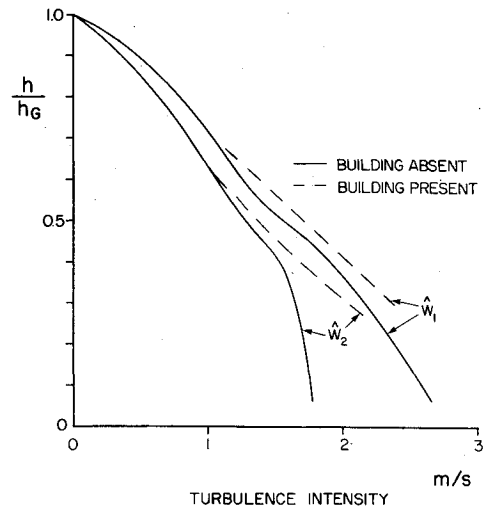

Fig. 1 Measured rms turbulence profiles.

where h is height above ground level, $W_G = 20.1$ m/s, and $h_G = 304.8$ m in the full-scale atmosphere. The boundary layer simulated conditions that exist over smooth open terrain under neutral atmospheric conditions in the presence of a strong wind.[6] A 152.4-m-tall office building and a steep (15 deg) glideslope were located in the wind field. The building was 38.1 m wide (in the y direction) and 25.4 m deep (in the x direction). The glideslope intersected the ground plane 38.1 m to the right (in the y direction) of the building vertical centerline and 181.7 m downwind (in the x direction) of the building vertical centerline. (In the wind tunnel the value for h_G was 0.91 m and the building model was 0.46 m tall. All quantities given in the remainder of this paper will be expressed as full-scale values.)

The measured turbulence intensity along the glideslope (expressed by turbulence root mean square as a percent of local mean wind velocity) is presented in Fig. 1. As expected, the presence of the building has resulted in an upward shift in turbulence levels, with the greatest increase occurring at heights below the top of the building ($h/h_G < 0.5$).

The turbulence correlation matrix $R(t_1,t_2)$ was measured along the glideslope using a pair of constant-temperature hot-wire anemometer probes. The experimental technique is described in Ref. 5. In this instance t_1 represents the time taken by the aircraft to reach the upper probe location from a starting point near the top of the boundary layer and t_2 the same for the lower probe location. Five upper probe locations were employed corresponding to heights ranging from 212 to 93 m. The values of τ were selected to be compatible with the STOL aircraft employed.

A sample plot of a measured element of $R(t_1,t_2)$ relating to the longitudinal aircraft degrees of freedom is presented in Fig. 2. Here the ijth element of $R(t_1,t_2)$ is

$$R_{W_iW_j}(\tau) = \overline{W_i(\tau_1,t)\,W_j(\tau_2,t+\tau)} \qquad i=1,2 \qquad j=1,2 \tag{8}$$

Figure 2 shows the measured results for the cases when the building is present and absent from the flowfield. The influence of the building was twofold: an increase in the value of $R_{W_2W_2}(0)$, and a more rapid falloff in $R_{W_2W_2}(\tau)$ with increasing $|\tau|$. The latter effect is caused by the presence of building-induced turbulence which tends to be of smaller scale than that present in the natural planetary boundary layer. (In the present case, the building width is about one-third of the longitudinal turbulence scale in the natural planetary boundary layer at a height above ground of 76 m.) Similar trends were observed for $R_{W_1W_1}(\tau)$. In the case of $R_{W_1W_2}(\tau)$, no obvious building-induced effects were found.

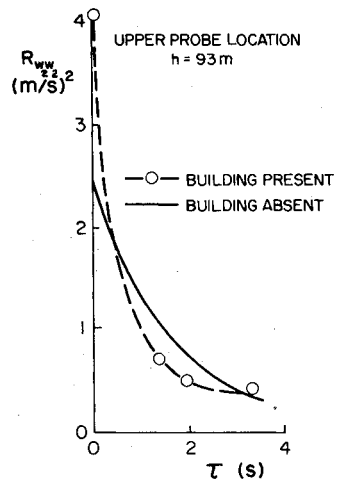

Fig. 2 Turbulence correlation $R_{W_2W_2}$.

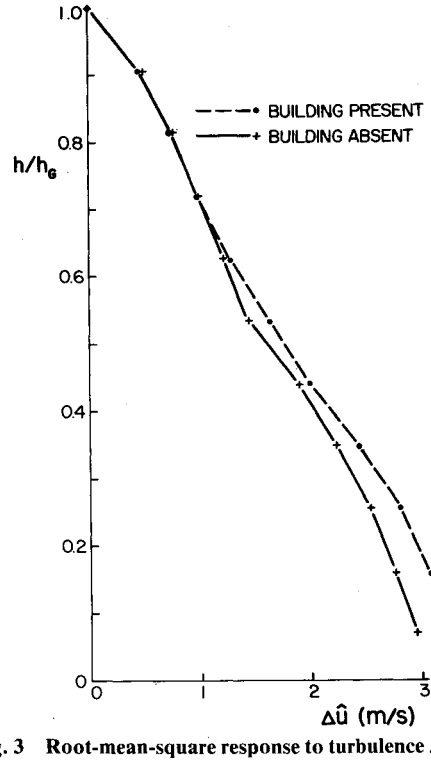

Fig. 3 Root-mean-square response to turbulence $\Delta\hat{u}$.

Computation of a STOL Aircraft's Response to Turbulence During the Landing Approach

The aircraft employed in this analysis was a twin-engine, turboprop light STOL transport (4994 kg) whose properties are described in Ref. 5. The reference equilibrium flight condition was a constant airspeed landing approach in the presence of a constant headwind. A fixed-controls case was employed in order to demonstrate the turbulence effects through aircraft state vector dispersions. (If an autopilot or human pilot model were used to close the control loop, then the effects of turbulence would best be studied by observing the control activity.)

The dispersions in the longitudinal state vector $\Delta x(t)$ at various locations along the glideslope were computed by implementing Eq. (3) on a digital computer. Typical results are plotted in Fig. 3, which presents the airspeed dispersion. The presence of the building resulted in a general increase in the predicted dispersions of the state vector with the extent of the increase becoming greater towards the bottom of the glideslope as the aircraft gets closer to the building. Thus, of the two effects that the building had on the shape of $R_{W_1W_1}(\tau)$ and $R_{W_2W_2}(\tau)$, it is seen that the increased values at $\tau=0$ dominate over the more rapid falloff with $|\tau|$. Based on the observed results, it appears that the presence of the upwind building has had only a minor impact on the turbulence-induced disturbance to the landing approach of the STOL transport.

Acknowledgments

This research has been supported by Environment Canada and the Natural Sciences and Engineering Research Council of Canada. The author would also like to acknowledge the assistance provided by P.S. Spedaler and W.O. Graf in gathering and processing the experimental data.

References

[1] Gerlach, O.H., van de Moesdijk, G.A.J., and van der Vaart, J.C., "Progress in the Mathematical Modelling of Flight in Turbulence," *Flight in Turbulence*, AGARD CP-140, 1973, pp. (S-1)-(S-38).

[2] Markov, A.B. and Reid, L.D., "A Review and Application of the Equivalent Deterministic Variable Technique: The Estimation of a STOL Aircraft's Response to Turbulence," University of Toronto, UTIAS Rept. 221, Feb. 1978.

[3] Markov, A.B., "The Landing Approach in Variable Winds: Curved Glidepath Geometries and Worst-Case Wind Modeling," University of Toronto, UTIAS Rept. 254, Dec. 1981.

[4] van der Vaart, J.C., "Worst-Case Wind Time Histories Causing Largest Deviations from a Desired Flight Path. An Analytical Approach," Delft University of Technology, Department of Aerospace Engineering, Rept. LR-267, April 1978.

[5] Reid, L.D., Etkin, B., Teunissen, H.W., and Hughes, P.C., "A Laboratory Investigation into Flight Path Perturbations During Steep Descents of V/STOL Aircraft," AFFDL-TR-76-84, Aug. 1976.

[6] Reid, L.D., "Correlation Model for Turbulence Along the Glide Path," *Journal of Aircraft*, Vol. 15, Jan. 1976, pp. 13-20.

[7] Reid, L.D., Markov, A.B., and Graf, W.O., "A Comparison of Techniques for Estimating STOL Aircraft Response to Low Altitude Turbulence," *Aeronautical Quarterly*, Vol. 28, Nov. 1977, pp. 278-292.

[8] Frost, W., Reddy, R., Crosby, W., and Camp, D.W., "C/STOL Flight in Wind Disturbed by the Presence of Buildings," *Journal of Aircraft*, Vol. 16, Dec. 1979, pp. 856-860.

AIAA 81-1712R

Turbulence Measurements in an Ejector Wing Flowfield

G. D. Catalano*
Louisiana State University, Baton Rouge, La.
H.E. Wright,† D.G. Stephens,‡ K.S. Nagaraja§
Wright Patterson Air Force Base, Ohio
and
R.E. Walterick¶
Georgia Institute of Technology, Atlanta, Ga.

Introduction

CONSIDER the principle of an ejector.[1] In the simplest case, coaxial jets are confined to a duct rather than to a

Presented as Paper 81-1712 at AIAA Aircraft Systems and Technology Conference, Dayton, Ohio, Aug. 11-13, 1981; submitted Dec. 14, 1981; revision received March 1, 1982.

*Assistant Professor of Mechanical Engineering. Member AIAA.
†Professor of Aeronautical Engineering, AFIT.
‡Graduate Assistant, AFIT/ENY.
§Senior Scientist, AFWAL/FIMM.
¶Research Scientist, School of Aerospace Engineering.